Cosmology from the integrated shear 3-point correlation function:

simulated likelihood analyses with machine-learning emulators

Zhengyangguang (Laurence) Gong (USM)

with: Anik Halder, Alex Barreira, Stella Seitz and Oliver Friedrich
https://arxiv.org/abs/2304.01187

GCCL seminar
05.05.2023

Integrated shear 3-point correlation functions

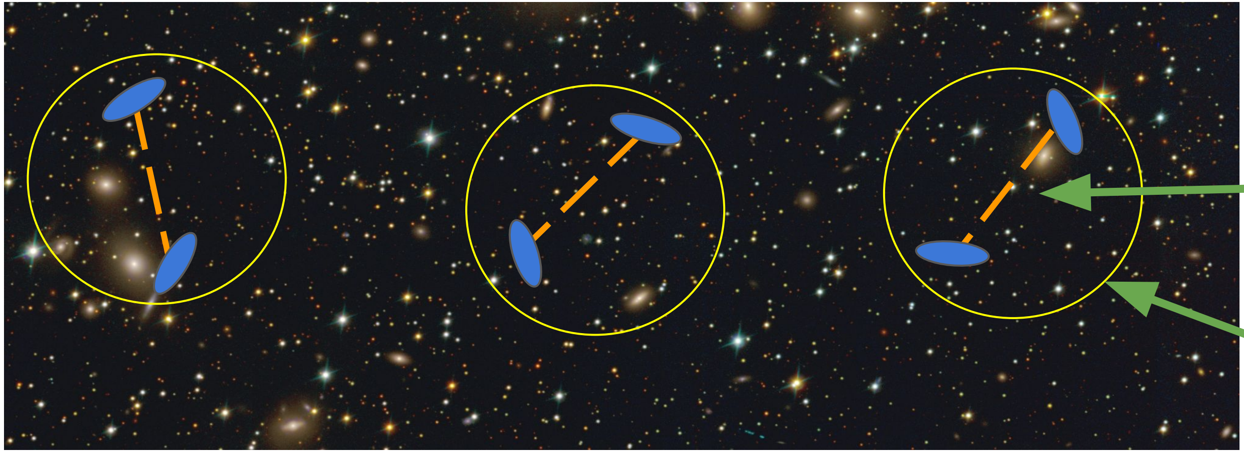

Position-dependent shear 2-pt correlation in top-hat aperture

$$\hat{\xi}_{\pm}(\theta; \boldsymbol{\theta_C})$$

Aperture mass

$$M_{\mathrm{ap}}(\boldsymbol{\theta_C})$$

Weighted tangential shear inside the filter

$$\zeta_{\pm}(\theta) \equiv \langle M_{\mathrm{ap}}(\boldsymbol{\theta_C})\, \hat{\xi}_{\pm}(\theta; \boldsymbol{\theta_C}) \rangle$$

$\rightarrow$ Directly observable higher-order statistic of the cosmic shear field

$\rightarrow$ Probes the line-of-sight projection of the 3D matter bispectrum

Halder et al. (2021)
arxiv:2102.10177

Theory prediction vs. N-body simulation

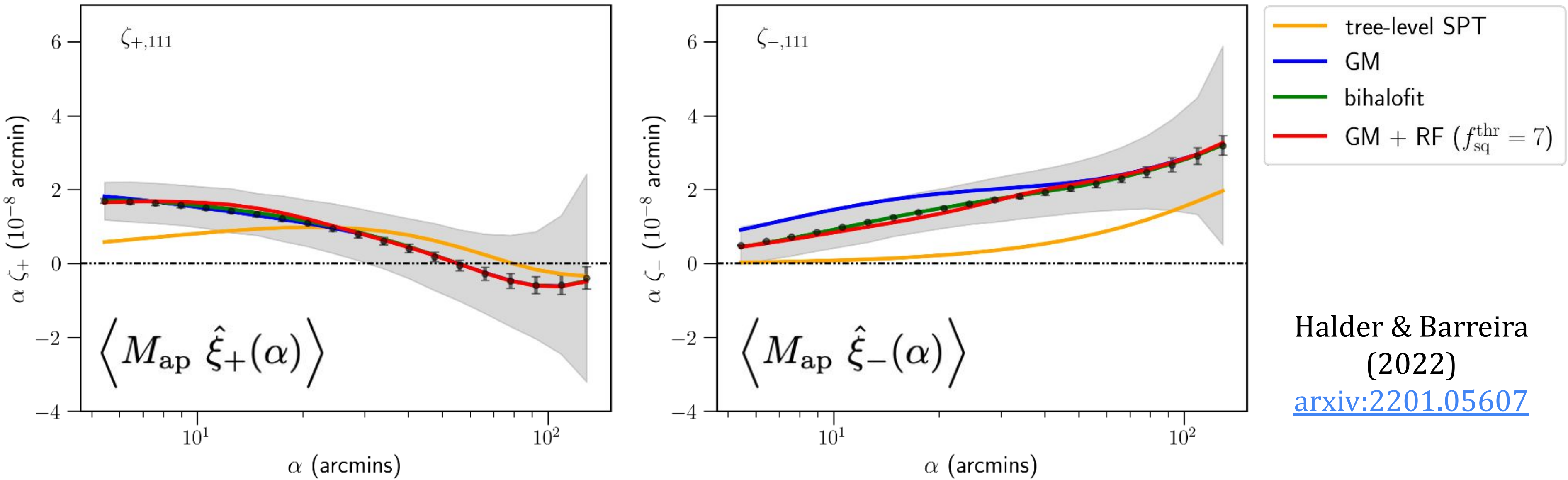

Halder & Barreira (2022)
[arxiv:2201.05607](https://arxiv.org/abs/2201.05607)

- **Response approach** (*Barreira & Schmidt 2017*) modelling of the integrated 3PCF (red curves → show good agreement to the T17 simulations)

- Encode baryonic feedback effects into integrated shear 3PCF

Theory prediction vs. N-body simulation

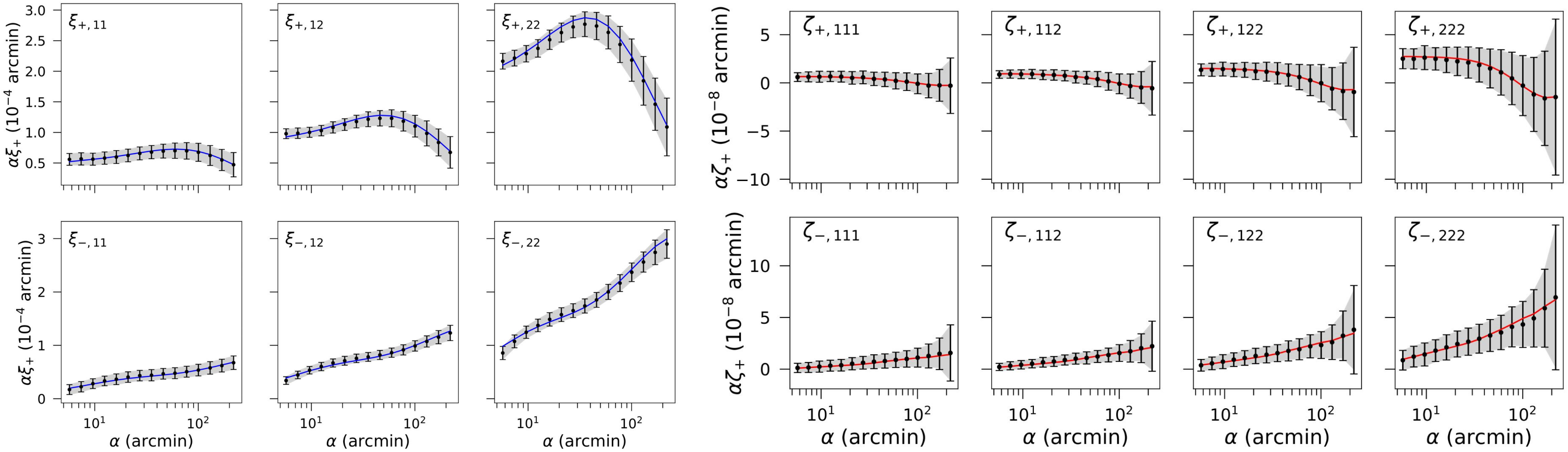

- Two DES Y3-like tomographic bins for both ξ± and ζ± (auto/cross-correlation)
- Theory prediction including response function approach to perturbation theory and baryonic feedback recipe in ζ±
- Simulation data points from 540 DES Y3-like footprints in 2017 Takahashi full-sky simulation arXiv:1706.01472

Emulation of integrated shear 3PCF and the modelling of systematic effects

Gong, Halder, Barreira, Seitz & Friedrich 2023 (arxiv:2304.01187)

Modelling the integrated shear 3PCF

$$\zeta_\pm(\alpha) = \left\langle \hat{M}_{\rm ap}(\boldsymbol{\theta}_C)\, \hat{\xi}_\pm(\alpha;\boldsymbol{\theta}_C) \right\rangle$$

$$= \frac{1}{A_{\rm 2pt}(\alpha)} \int \frac{\mathrm{d}\ell\, \ell}{2\pi}\, \mathcal{B}_\pm(\ell) J_{0/4}(\ell\alpha)$$

Compensated filter

Top-hat filter

$$\mathcal{B}_\pm(\ell) = \int \mathrm{d}\chi\, \frac{q_\kappa^3(\chi)}{\chi^4} \int_{\boldsymbol{\ell}_1} \int_{\boldsymbol{\ell}_2} B_\delta^{\rm 3D}\left(\frac{\boldsymbol{\ell}_1}{\chi}, \frac{\boldsymbol{\ell}_2}{\chi}, \frac{-\boldsymbol{\ell}_{12}}{\chi}; \chi\right) e^{2i(\phi_{\boldsymbol{\ell}_2} \mp \phi_{-\boldsymbol{\ell}_{12}})} U(\boldsymbol{\ell}_1) W(\boldsymbol{\ell}_2 + \boldsymbol{\ell}) W(-\boldsymbol{\ell}_{12} - \boldsymbol{\ell})$$

Line-of-sight projection

3D matter bispectrum

Window functions

Emulation

- Emulate the 4-dimensional integration which is computationally expensive
- Leaving the line-of-sight projection out of emulation: Preserving the flexibility in the systematic modelling

Emulate the integrated bispectrum using neural network (NN)

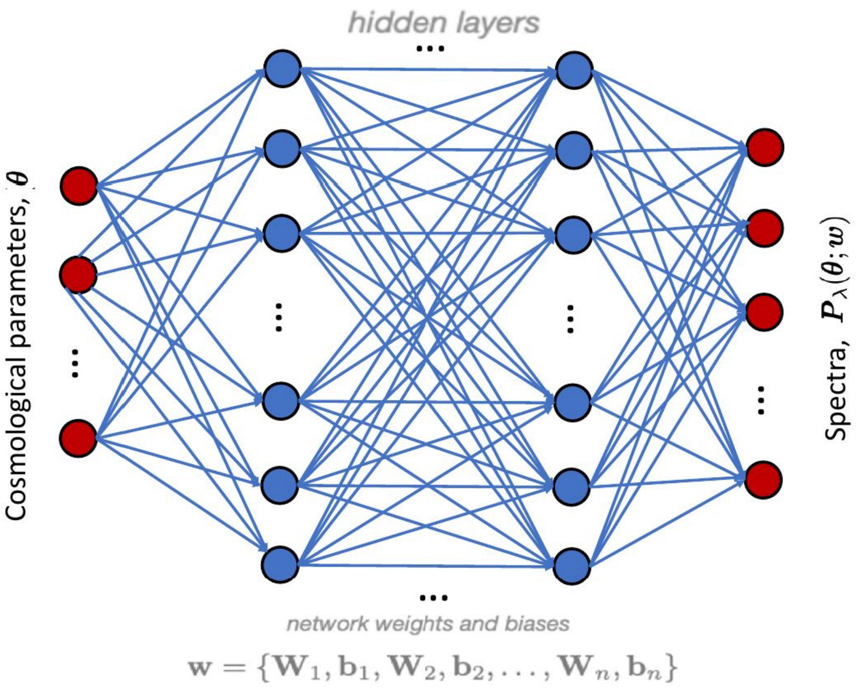

Mancini et al. (2021)
arXiv:2106.03846

- The emulator is constructed using the package containing a suite of fully connected NN: Cosmopower

- Cosmopower:

  training feature: $\{\Omega_m, \ln(10^{10}A_s), w_0, c_{\min}, z\}$

  training label: pre-computed spectra at 100 multipoles

  training on GPU

- Each emulator is for a specific filter size:

  100000 training nodes (10% validation)

  1000 testing nodes

Data preparation and pre-processing

	Prior range
Cosmological parameters (emulated)	
Ω_{m}	$U\,[0.16, 0.45]$
$\ln(10^{10} A_s)$	$U\,[1.61, 4.20]$
w_0	$U\,[-3.33, -0.33]$
Baryonic feedback parameter (emulated)	
c_{min}	$U\,[1.0, 5.5]$
Systematic parameters (not emulated)	
Δz_1	$\mathcal{N}(0.0, 0.023)$
Δz_2	$\mathcal{N}(0.0, 0.020)$
m_1	$\mathcal{N}(0.0261, 0.012)$
m_2	$\mathcal{N}(-0.061, 0.011)$
$A_{\mathrm{IA},0}$	$U\,[-5.0, 5.0]$
α_{IA}	0 (fixed)

With the additional emulated parameter redshift z between 0.0 and 2.0

- Emulation prior:

  <u>Too wide</u>: 1. a waste of training data;
  2. Labels can experience numerical instability or give unusual predictions that form prominent outliers

  <u>Too narrow</u>: Parameter inference will be dominated by priors

- Scale primordial power spectrum amplitude logarithmically;
  Scale the training labels: integrated bispectrum and matter power spectrum with log10

Emulation accuracy test

$$\epsilon \equiv \left| \frac{\chi^2_{\mathrm{emu},i}}{\chi^2_{\mathrm{test},i}} - 1 \right|$$

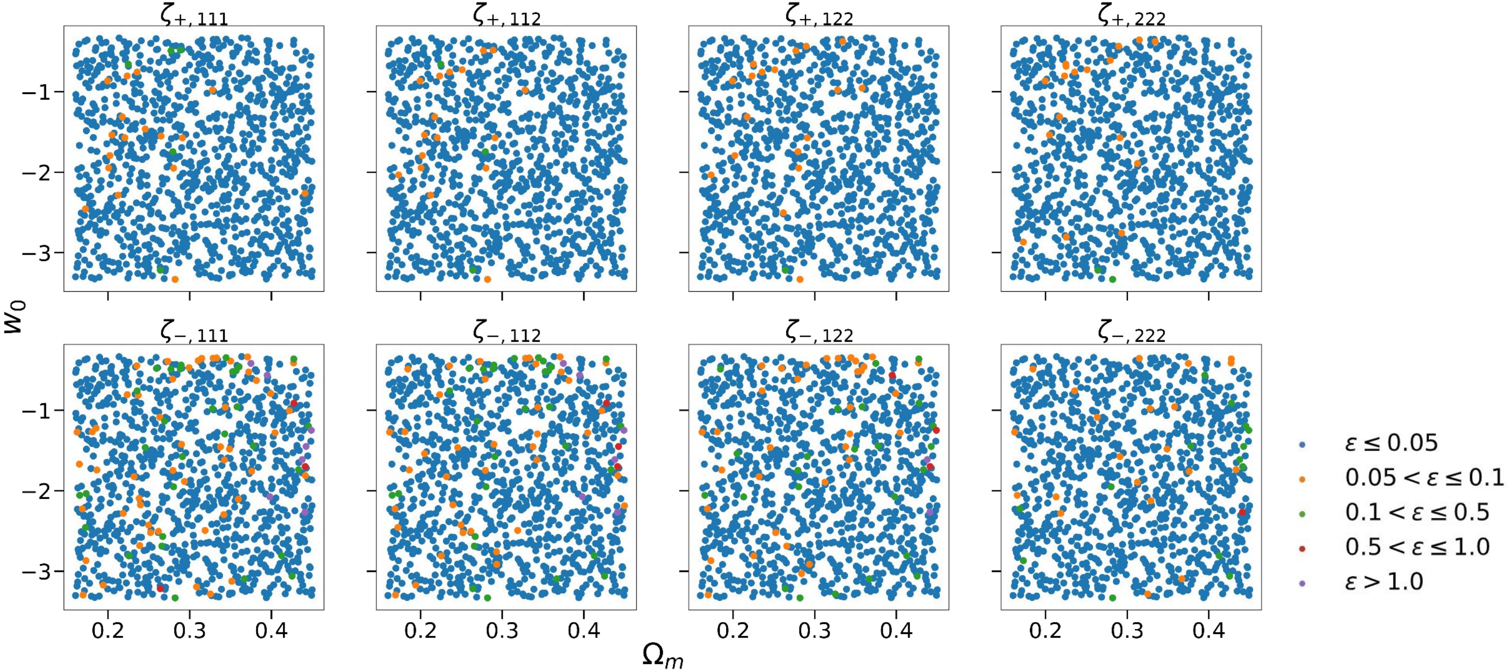

- All 8 non-redundant integrated shear 3PCF from 2 DES Y3-like tomographic bins
- Using chi2 fractional difference as the emulation accuracy metric: It describes how closely the emulators describe the log-likelihood surface w.r.t the theory model predictions

Including other weak lensing systematics

- **Photometric redshift uncertainty**

$$n_s^i(z) = \hat{n}_s^i(z + \Delta z^i)$$

- **Multiplicative shear bias**

$$\xi_{\pm,ij}(\alpha) \longrightarrow (1+m_i)(1+m_j)\xi_{\pm,ij}(\alpha) \ ,$$
$$\zeta_{\pm,ijk}(\alpha) \longrightarrow (1+m_i)(1+m_j)(1+m_k)\zeta_{\pm,ijk}(\alpha)$$

- **Intrinsic alignment** (non-linear linear alignment (NLA) model)

$$q^i(\chi) \longrightarrow q^i(\chi) + f_{\rm IA}(z(\chi))\frac{n_s^i(\chi)}{\bar{n}_s^i}\frac{\mathrm{d}z}{\mathrm{d}\chi} \qquad f_{\rm IA}(z) = -A_{\rm IA,0}\left(\frac{1+z}{1+z_0}\right)^{\alpha_{\rm IA}}\frac{c_1\rho_{\rm crit}\Omega_{\rm m,0}}{D(z)}$$

- We do not include these components in the emulation so that the flexibility enables others to adopt different models

Covariance estimation

Covariance estimation I

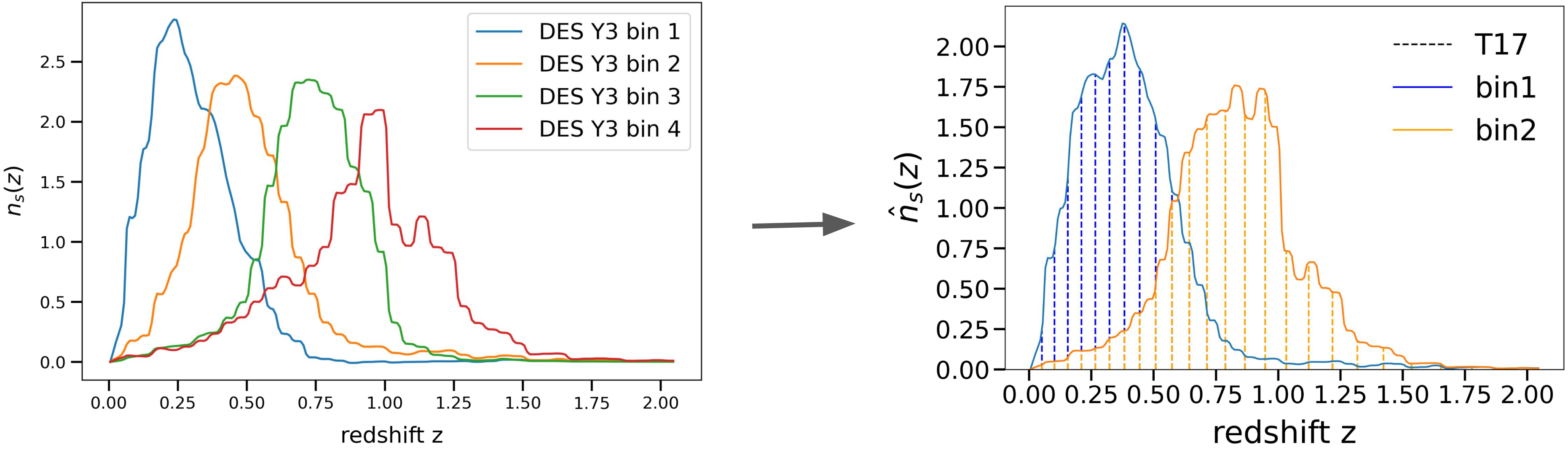

- We merge 4 DES Y3 source redshift bins into 2 via a weighted summation
- Increase the signal-to-noise ratio of the integrated shear 3PCF

Covariance estimation II

5 rotated DES Y3-like footprints

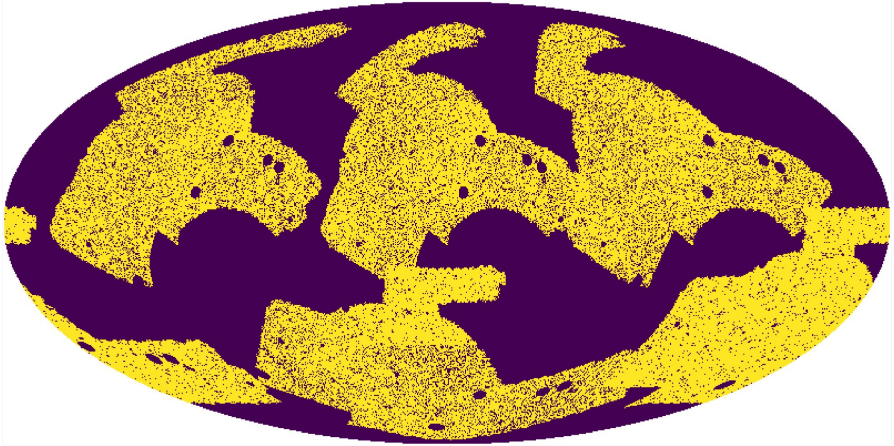

- Superimpose the DES Y3 footprint onto the full sky simulation map and rotate it to five non-overlapping locations

- Add shape noise following the equation:

$$\gamma_{\rm pix} = \gamma_{\rm noise} + \gamma_{\rm sim} = \frac{\sum_{j=1}^{N} \omega_j \gamma_{j,\rm DES} \exp(i\phi_j)}{\sum_{j=1}^{N} \omega_j} + \gamma_{\rm sim}$$

- Select mass apertures that have enough number of valid pixels

- Estimate data covariance from both N-body T17 simulation and FLASK log-normal maps

Results of simulated likelihood analyses

- Validation on the T17 cosmic shear maps
- The impact of the aperture size
- The impact of systematics and their modelling
- The impact of different covariance estimates

Validation on the T17 cosmic shear maps

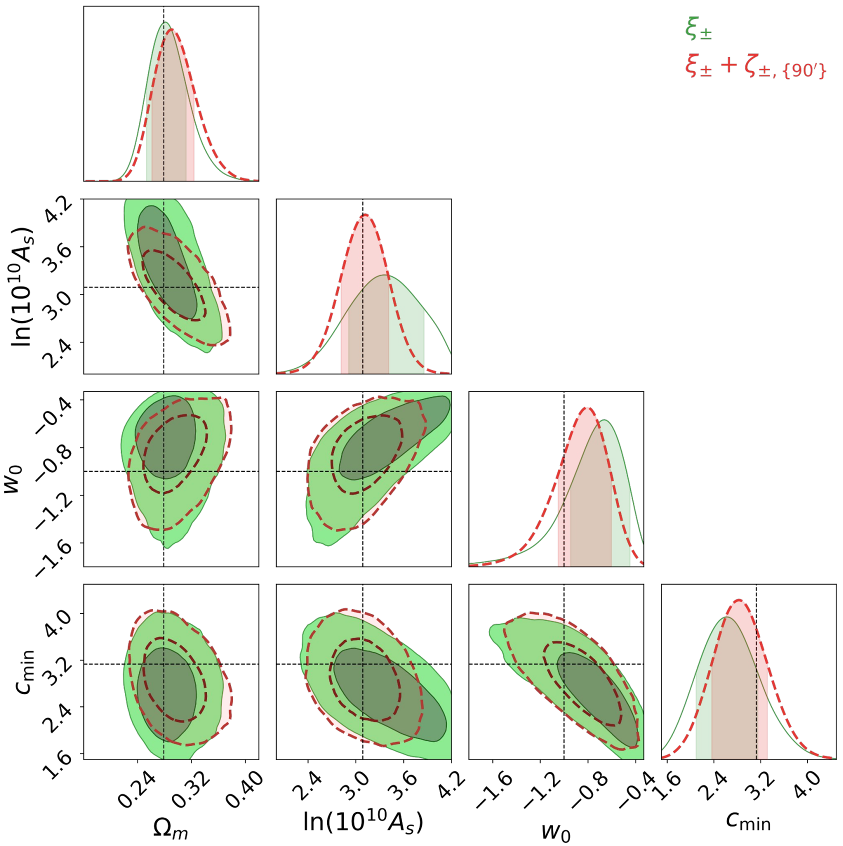

- The data vector comes from the average over 540 DES Y3-like footprints on T17 shear maps (Takahashi et al (2017), arXiv:1706.01472)
- The data covariance matrix is estimated from 1500 DES Y3-like footprints on FLASK log-normal shear maps
- The inferred parameter covariance is not biased from the fiducial T17 cosmological parameter values

The impact of the aperture size

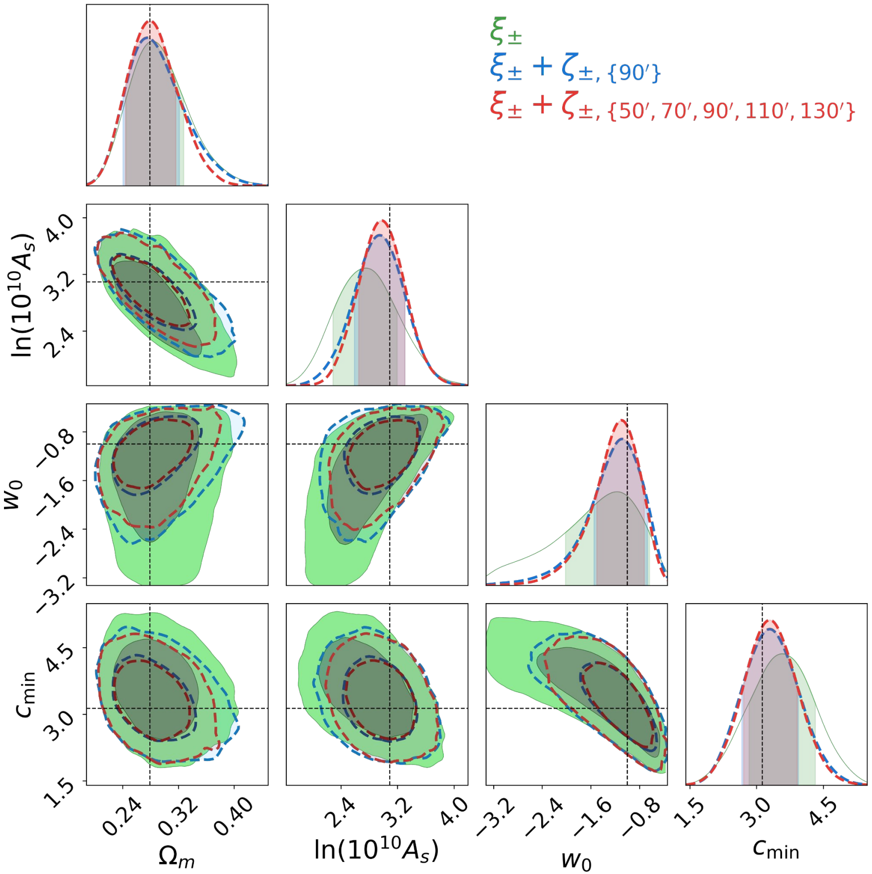

- We train 5 emulators for integrated shear 3PCF with different filter sizes: {50', 70', 90', 110', 130'}
- Marginalized over systematic parameters – photo-z, shear bias and intrinsic alignment (NLA) parameters

Aperture sizes (arcmin)	Ω_m	$\ln(10^{10}A_s)$	w_0	$c_{\min}$
50	1.2%	9.0%	18.1%	4.8%
70	1.2%	16.9%	31.9%	11.6%
90	**3.7%**	**20.2%**	**38.4%**	**15.1%**
110	1.2%	19.1%	34.1%	11.0%
130	1.2%	16.9%	32.6%	12.3%
{50, 70, 90}	2.5%	24.7%	39.1%	15.8%
{50, 90, 130}	3.7%	23.6%	41.3%	16.4%
{70, 90, 110}	6.2%	25.8%	39.1%	15.1%
{90, 110, 130}	8.6%	25.9%	42.8%	15.8%
{50, 70, 90, 110, 130}	**12.4%**	**28.1%**	**44.9%**	**19.9%**

The impact of systematics and their modelling

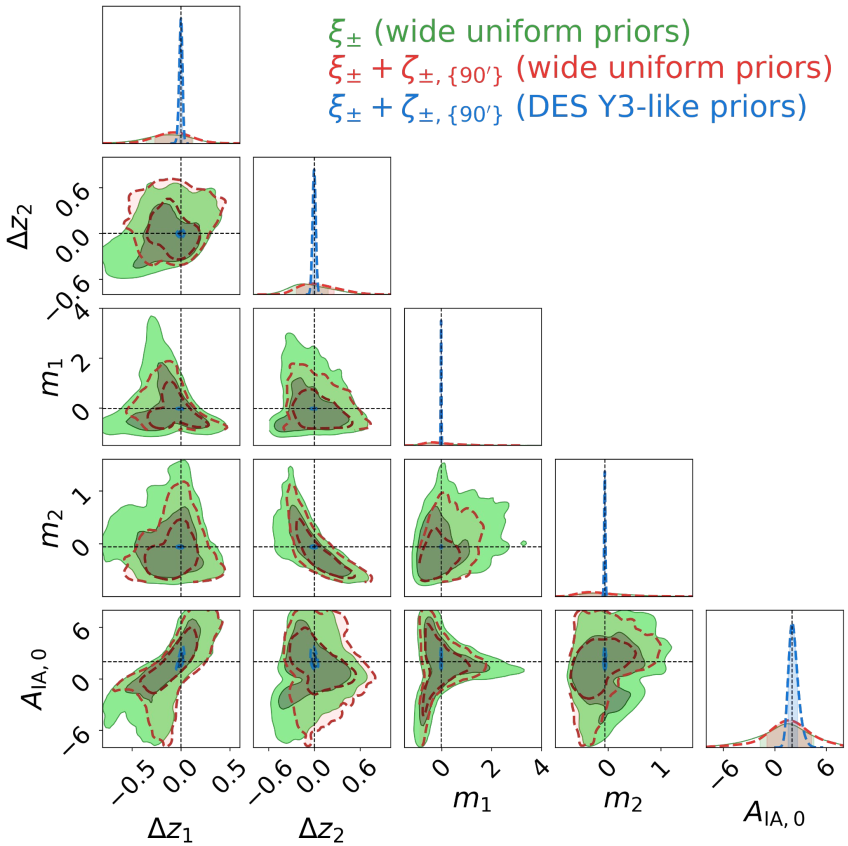

- Idea: 2-point and 3-point statistics depend differently on systematic parameters $\rightarrow$ Self-calibration of systematic parameters that can reduce the need for external calibration data

- Quantitatively it is in contrast with the results reported in the work Pyne & Joachimi (2021) arXiv: 2010.00614 for an Euclid-like survey setups

The impact of systematics and their modelling

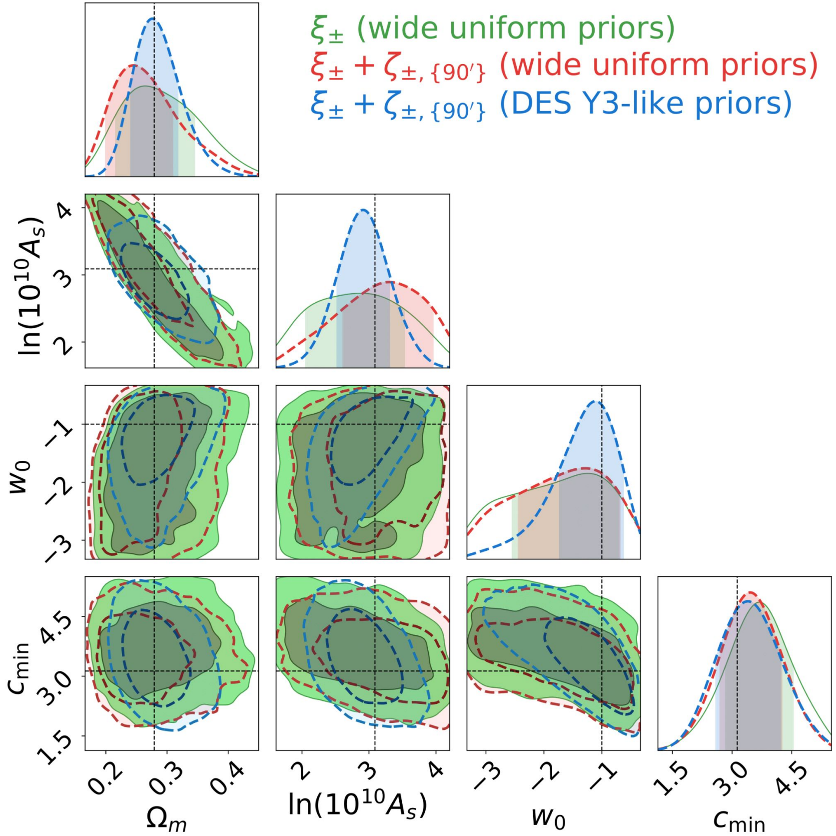

- Same wide priors on nuisance parameters; Cosmological parameter constraints by adding ζ±

- Adding ζ± to ξ± does not prevent the degradation of parameter constraints as significantly as predicted in arXiv: 2010.00614

The impact of different covariance estimates

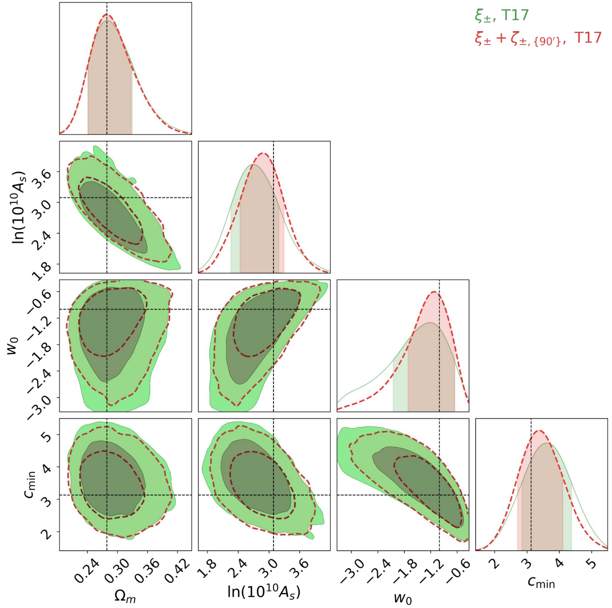

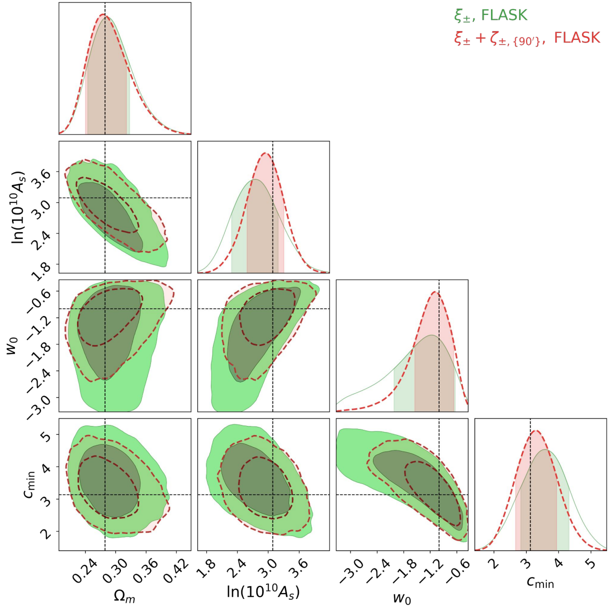

- FLASK-based covariance may not be suitable to cosmological constraints using 3-point cosmic shear information
- Real-data analyses may require using more expensive N -body simulations, or calculating the covariance matrix analytically

Covariance type	$\Omega_{\rm m}$	$\ln\left(10^{10}A_s\right)$	w_0	$c_{\rm min}$
FLASK (lognormal)	3.7%	20.2%	38.4%	15.1%
T17 (N-body simulations)	3.5%	8.8%	26.1%	8.7%

Summary

- Our analysis pipeline is accurate and able to yield unbiased parameter constraints from our N -body simulation DES Y3-like data vectors.

- Aperture size 90 arcmin is what results in the largest information gain from $\zeta_\pm$. The combination of several filter sizes can improve the constraints further but at the cost of dealing with a larger data vector and covariance matrix.

- We do not find significant improvements of systematic constraints in combined $\xi_\pm + \zeta_\pm$ analyses; i.e. the mitigation of systematic effects still requires prior calibration from external data

- Lognormal realizations might not provide reliable estimates of the $\zeta_\pm$ covariance matrix.

- The next step is to apply this higher-order statistic pipeline to DES Y3 data and extract cosmological information

Thank you!

Additional slides

Responses in large-scale structures

- For details please refer to Barreira & Schmidt 2017 [arXiv: 1703.09212](https://arxiv.org/abs/1703.09212)

- Non-SPT method to compute higher-order correlation function in squeezed limit into nonlinear regime via nonlinear matter power spectrum and different orders of responses $\mathcal{R}_n$

- Squeezed limit configuration:

$$\langle \delta(\boldsymbol{k})\delta(\boldsymbol{k}')\delta(\boldsymbol{p}_1)\delta(\boldsymbol{p}_2)\cdots\delta(\boldsymbol{p}_n)\rangle_c\,, \quad \text{with} \quad p_i \ll k, k' \;(i = 1, 2, \cdots, n) \text{ and } p_{12..n} \ll k, k'$$

- Responses in 3-point correlation function [(n+2)-point correlation function linked to nth order response]

$\lim_{p\to 0}$ (

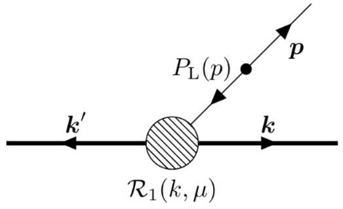

$+ (\boldsymbol{k} \leftrightarrow \boldsymbol{k}')$) $= \mathcal{R}_1(k; \mu_{\boldsymbol{k},\boldsymbol{p}}) P_m(k) P_{\rm L}(p)\, (2\pi)^3 \delta_D(\boldsymbol{k} + \boldsymbol{k}' + \boldsymbol{p})$

Including other weak lensing systematics

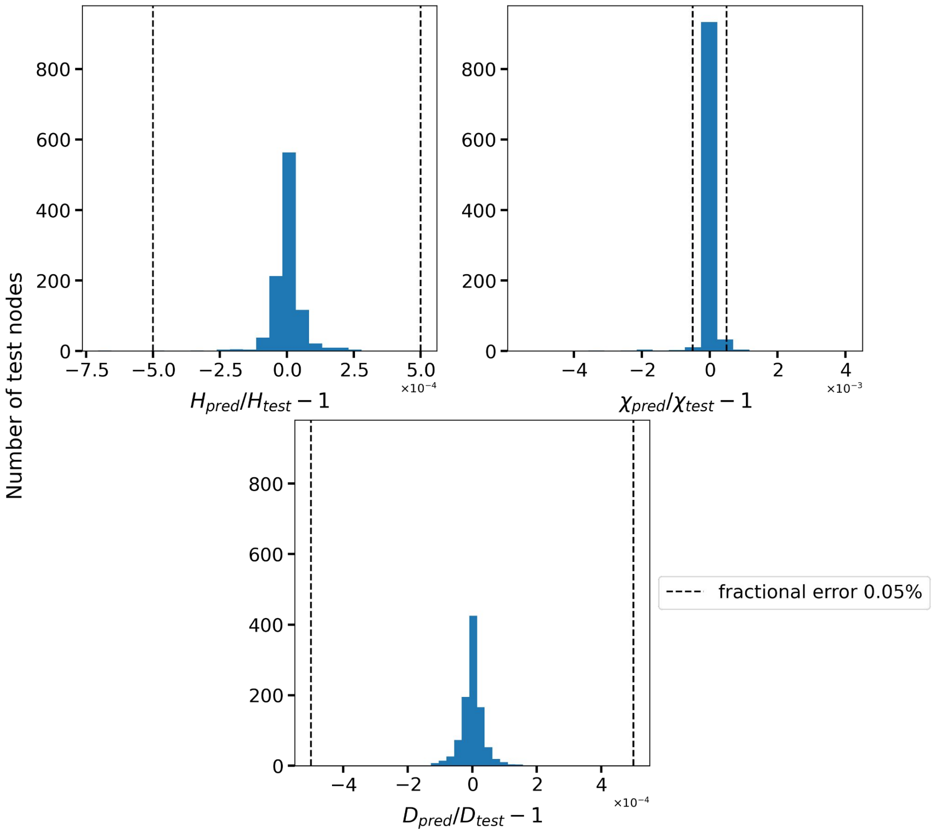

- The emulator is constructed using the package exploiting Gaussian Process: GPflow (de G. Matthews et al (2016) arXiv:1610.08733)
- GPflow:

  training feature: $\{\Omega_{\rm m}, A_s, w_0, z\}$

  training label: H, chi or D (growth factor)

  training on GPU
- 10000 training nodes

  1000 testing nodes

Intrinsic alignment modelling in power spectrum and bispectrum

- Illustratively the 2-point correlation of weak lensing shear:

  $$\xi^{ij}_{\pm,\mathrm{obs}} = \xi^{ij}_{\pm,\mathrm{GG}} + \xi^{ij}_{\pm,\mathrm{GI}} + \xi^{ij}_{\pm,\mathrm{IG}} + \xi^{ij}_{\pm,\mathrm{II}}$$

  The relation between different power spectrum terms and the NLA kernel:

  $\propto f^0_{\mathrm{IA}}$ (GG), $\propto f_{\mathrm{IA}}$ (GI, IG) and $\propto f^2_{\mathrm{IA}}$ (II)

- Contributions to the integrated shear 3-point correlation function:

  $$\zeta^{ijk}_{\pm,\mathrm{obs}} = \zeta^{ijk}_{\pm,\mathrm{GGG}} + \zeta^{ijk}_{\pm,\mathrm{GGI}} + \zeta^{ijk}_{\pm,\mathrm{GIG}} + \zeta^{ijk}_{\pm,\mathrm{GII}} + \zeta^{ijk}_{\pm,\mathrm{IGG}} + \zeta^{ijk}_{\pm,\mathrm{IGI}} + \zeta^{ijk}_{\pm,\mathrm{IIG}} + \zeta^{ijk}_{\pm,\mathrm{III}}$$

  The relation between different bispectrum terms and the NLA kernel:

  $\propto f^0_{\mathrm{IA}}$ (GGG), $\propto f_{\mathrm{IA}}$ (GGI, GIG, IGG) and $\propto f^2_{\mathrm{IA}}$ (GII, IGI, IIG) and $\propto f^3_{\mathrm{IA}}$ (III)

Intrinsic alignment modelling in power spectrum and bispectrum

Pyne & Joachimi (2021) arXiv: 2010.00614

- $$P_{\delta\delta_{\rm I}}(k) = f_{\rm IA} P_{\rm NL}(k),$$

  $$P_{\delta_{\rm I}\delta_{\rm I}}(k) = f_{\rm IA}^2 P_{\rm NL}(k)$$

- $$\begin{aligned} B_{\delta\delta\delta_{\rm I}}(\boldsymbol{k}_1, \boldsymbol{k}_2, \boldsymbol{k}_3) = 2\big[& f_{\rm IA}^2 F_2^{\rm eff}(\boldsymbol{k}_1, \boldsymbol{k}_2) P_{\rm NL}(k_1) P_{\rm NL}(k_2) \\ & + f_{\rm IA} F_2^{\rm eff}(\boldsymbol{k}_2, \boldsymbol{k}_3) P_{\rm NL}(k_2) P_{\rm NL}(k_3) \\ & + f_{\rm IA} F_2^{\rm eff}(\boldsymbol{k}_3, \boldsymbol{k}_1) P_{\rm NL}(k_3) P_{\rm NL}(k_1)\big] \end{aligned}$$

  $$\begin{aligned} B_{\delta\delta_{\rm I}\delta_{\rm I}}(\boldsymbol{k}_1, \boldsymbol{k}_2, \boldsymbol{k}_3) = 2\big[& f_{\rm IA}^3 F_2^{\rm eff}(\boldsymbol{k}_1, \boldsymbol{k}_2) P_{\rm NL}(k_1) P_{\rm NL}(k_2) \\ & + f_{\rm IA}^2 F_2^{\rm eff}(\boldsymbol{k}_2, \boldsymbol{k}_3) P_{\rm NL}(k_2) P_{\rm NL}(k_3) \\ & + f_{\rm IA}^3 F_2^{\rm eff}(\boldsymbol{k}_3, \boldsymbol{k}_1) P_{\rm NL}(k_3) P_{\rm NL}(k_1)\big], \end{aligned}$$

  $$B_{\delta_{\rm I}\delta_{\rm I}\delta_{\rm I}}(\boldsymbol{k}_1, \boldsymbol{k}_2, \boldsymbol{k}_3) = f_{\rm IA}^4 B_{\delta\delta\delta}(\boldsymbol{k}_1, \boldsymbol{k}_2, \boldsymbol{k}_3).$$

Cosmic shear 2-point correlation functions

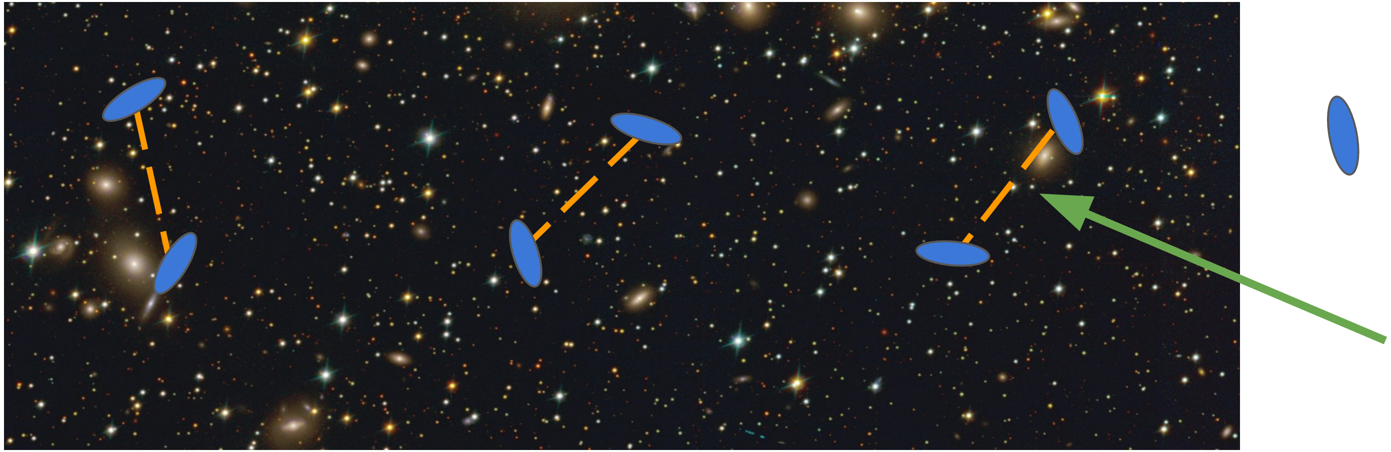

Background source galaxy ellipticity

$$\hat{\xi}_{\pm}(\theta)$$

Shear 2-point correlation functions

→ Probes the line-of-sight projection of the 3D matter power spectrum

→ But cosmic shear is a non-Gaussian field with information beyond 2-point correlations!

Emulation for shear 2PCF

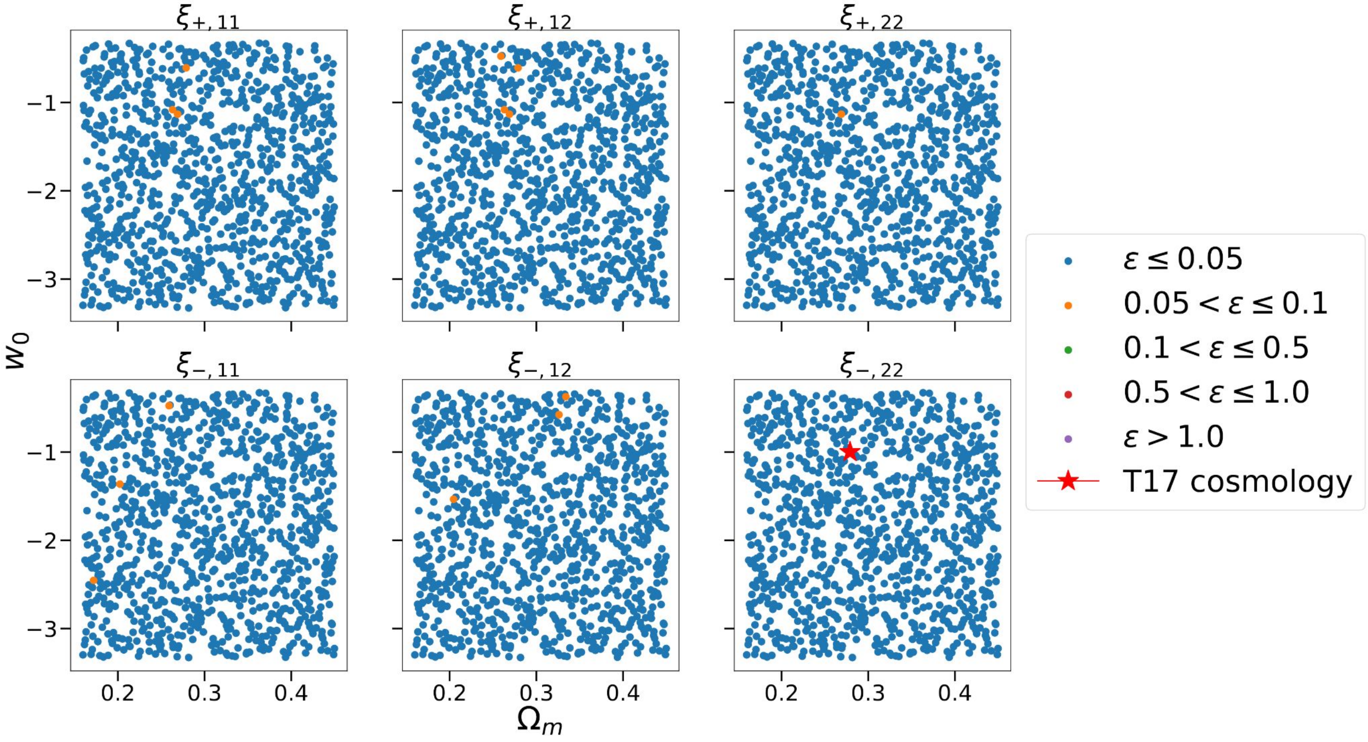

- All 6 shear 2PCFs from 2 DES Y3 tomographic bins

Simulated DESY3 MCMCs with 2PCF and integrated 3PCF

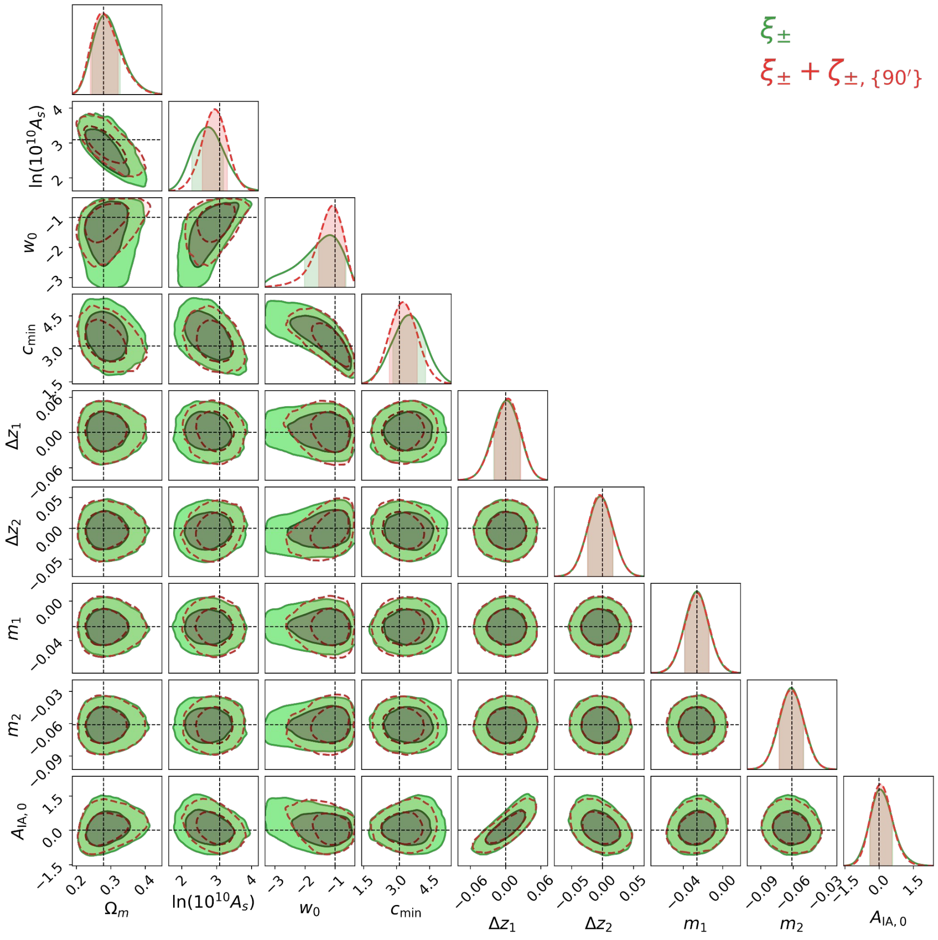

- Green: shear 2PCF only
  Red: shear 2PCF & integrated shear 3PCF (*for a single filter size*)
- MCMC on GPU: using emcee affine invariant sampler and sample **million points in ~ 1 hour**
- The inferred systematic parameter covariance is dominated by the corresponding DES Y3 gaussian priors

T17 vs. FLASK

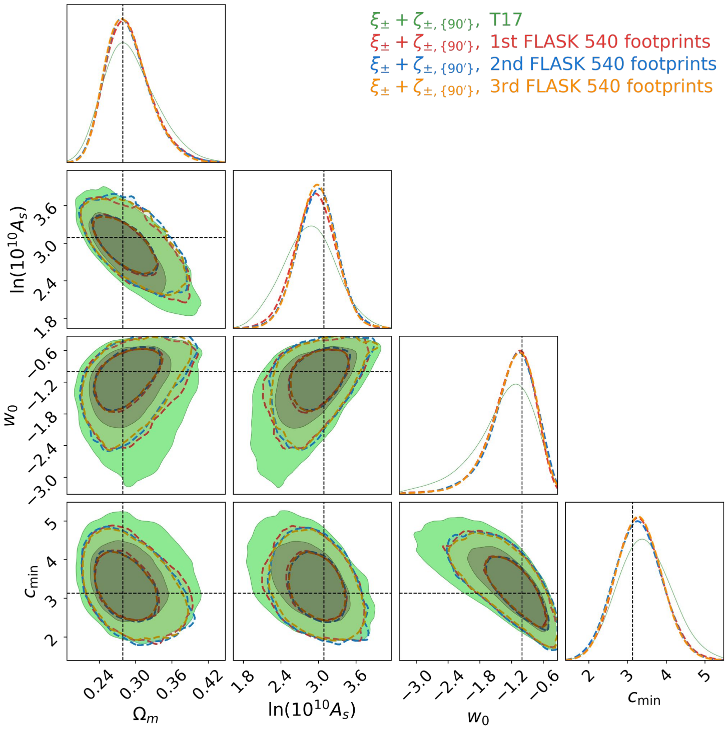
$\xi_\pm + \zeta_{\pm,\{90'\}}$, T17
$\xi_\pm + \zeta_{\pm,\{90'\}}$, 1st FLASK 540 footprints
$\xi_\pm + \zeta_{\pm,\{90'\}}$, 2nd FLASK 540 footprints
$\xi_\pm + \zeta_{\pm,\{90'\}}$, 3rd FLASK 540 footprints
Ω_m
$\ln(10^{10}A_s)$
w_0
$c_{\min}$

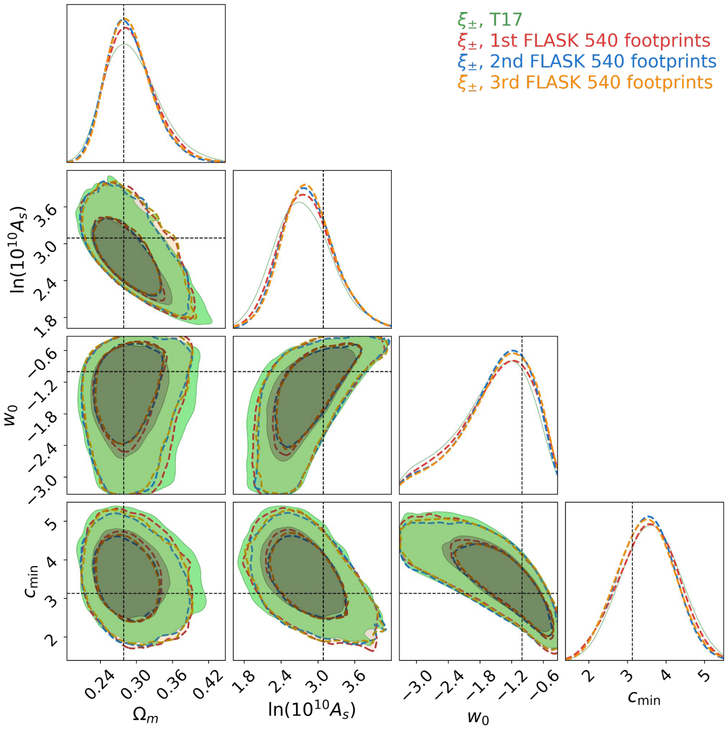
$\xi_\pm$, T17
$\xi_\pm$, 1st FLASK 540 footprints
$\xi_\pm$, 2nd FLASK 540 footprints
$\xi_\pm$, 3rd FLASK 540 footprints
Ω_m
$\ln(10^{10}A_s)$
w_0
$c_{\min}$